

Enhancing precision in agriculture: A smart predictive model for optimal sensor selection through IoT integration



Praveen Sankarasubramanian

Founder, RMD Research labs, Chennai, Tamil Nadu 600100, India

ARTICLE INFO

Keywords:
 Precision agriculture
 IoT sensor
 Node deployment
 Environmental condition
 Production yield rate

ABSTRACT

The rapid advancement in communication technology has sparked a transformative wave across various domains, significantly enhancing comfort and convenience in daily life. Addressing the escalating global demand for food, coupled with the need to alleviate the efforts of farmers, technology, particularly the Internet of Things (IoT), has emerged as a pivotal force. Precisely predicting variations in climate, ground conditions, and dirt attributes has emerged as a formidable challenge in the realm of agricultural IoT. In this paper, we introduce a smart optimal prediction model for sensors based on IoT-enabled precision agriculture. Initially, we enhance the THAM index (temperature, humidity, air- and water-quality measurement) by using the modified Wild Geese (MWG) algorithm to predict environmental conditions accurately. The deployment of IoT sensor nodes using quantum deep reinforcement learning (QDRL) to determine the ideal amount of devices required for effective coverage of the target agricultural field to improving communication. Furthermore, we compute the production yield rate, consider various attributes such as fertilizer regulatory measures, temperature quotient, and agronomy by using the improved prairie dog optimization (IPDO) algorithm. Finally, we assess the performance of MWG-QDRL-IPDO model using test samples collected from the Meteorology Bureau through the related sensor middleware. Our findings reveal a checking efficacy of 96.35 %, even with a reduced amount of devices covering a huge zone. Similarly, the accuracy of IoT sensor node deployment reaches 91.47 %, contributive to reduce the irrelevant data generation and processing time.

1. Introduction

A cutting-edge agricultural monitoring system harnesses the power of the internet of things (IoT) [1], sensors, and analytics to effectively oversee, optimize, and sustain agricultural practices. This innovative technology conducts a thorough examination of various factors including weather conditions, crop development, nutrient levels and soil moisture, to provide timely notifications to farmers [2]. The implementation of IoT in farming facilitates real-time data gathering, transmission, and analysis, empowering farmers with valuable insights for enhanced decision-making [3]. Intelligent farming observing systems utilize historical data and machine learning algorithms to forecast crucial elements like weather patterns, disease occurrences, and insect outbreaks [4,5]. IoT is used in agriculture to monitor crops, diagnose illnesses, anticipate yields, and use robotics for harvesting differing wireless connections with differing range, the bandwidth, and topologies make WSNs possible [6,7]. When linked to the edge gateways layer, all sensor node data is retained and processed for further analysis [8]. Technological solutions to farmers' issues of maximizing yields and

decreasing resource losses have increased in recent years [9]. Traditional soil nitrogen testing and crop recommendations are arduous and subjective [10,11]. Due to this, farmers often make poor decisions that increase their environmental impact, lower yields, and squander resources [12]. These limits must be addressed using innovative approaches that give real-time soil nutrient data and personalized crop suggestions [13]. Data collection, analysis, and automation have been greatly improved by the IoT in agriculture [14]. Due to data formats, communication protocols, and manufacturers, agricultural IoT systems and equipment are incompatible [15]. Lack of compatibility can hinder data transfer and collaboration across IoT parties, making it harder to integrate diverse IoT devices into a unified ecosystem [32,33]. To manage IoT data quantities, big data analytics, machine learning, and data visualization are needed [16]. These technologies enable IoT data collection, storage, analysis, and comprehension that is safe, scalable, and effective [17]. Agriculture researchers and farmers struggle to manage the massive IoT statistics [18]. The IoT in farming is hard and expensive due to device maintenance and configuration changes [19]. Farmers and agricultural professionals must evaluate the long-term

E-mail address: praveengrb@gmail.com.

<https://doi.org/10.1016/j.atech.2024.100749>

Received 3 February 2024; Received in revised form 12 June 2024; Accepted 1 October 2024

Available online 29 December 2024

2772-3755/© 2025 The Author. Published by Elsevier B.V. This is an open access article under the CC BY-NC-ND license (<http://creativecommons.org/licenses/by-nc-nd/4.0/>).

sustainability and cost of the IoT based on jobs, ownership of data, and technology dependence [20]. IoT deployment raises social and ethical issues that must be considered. MWG-QDRL-IPDO is smart optimum predictive model for sensor in IoT-enabled precision farming which makes numerous notable advances to agricultural efficiency and precision. The main contributions of our work:

1. We employ the modified wild geese (MWG) method to optimize the THAM index, enabling reliable environmental predictions for agricultural management.
2. Our approach prioritizes the strategic placement of IoT sensor nodes. Quantum deep reinforcement learning (QDRL) is used to determine the optimal number of sensors required to effectively monitor the target agricultural area.
3. The model evaluates and enhances efficiency by determining the output rate, considering factors such as fertilizer regulation, temperature, and agronomy. The improved prairie dog optimization (IPDO) algorithm is utilized to optimize these specific properties.

The rest of this paper is organized as follows. Section 2 describes the review of literature related to the IoT enabled precision agriculture. The overview of proposed methodology is discussed in Section 3. The THAM index optimization is discussed in Section 4, the node deployment and production yield rate computation is discussed in Section 5 and 6, respectively. The results and comparative analysis is discussed in Section 7. Finally, the paper concludes in Section 8.

2. Related work

This section provides a review of the literature pertaining to IoT-enabled precision agriculture. It encompasses an overview of key studies and findings in the field, focusing on the integration of IoT technologies to enhance precision and efficiency in agricultural practices.

Agrawal et al. [21] proposed precision farming enabled by the IoT to predict the accumulated energy consumption at the base station. The demand component consists of resources linked to the station base, such sensors and pathways and the source component is the electrical power stored by the extraction modules. The product density model, known for its effectiveness in capturing time-dependent random variations, is used for IoT-enabled base stations in precision agriculture, with potential applications in other IoT systems. Jayalakshmi et al. [22] conducted an analysis on the impact of soil temperature and soil water suction on the growth rate and speed of wheat seeds. The study involved planting and cultivating wheat seeds in non-adsorbing material created by sand grains at elevated temperatures. The findings emphasize the need for approaches tailored to smaller-scale farms and capable of capturing information at each step of the process, as existing solutions designed for mechanized manufacturing may not be suitable. Gsangaya et al. [23] have introduced an enhanced agriculture monitoring system that addresses shortcomings present in precedingschemes, withprice, attentionvariety, and outside usability. The system is characterized by its simplicity, low cost, wireless capability, and suitability for outdoor use, making it highly portable and robust. It operates on generated power, eliminating the need for extensive cabling, and offers added functionality to decrease agricultural workload and enhance crop yield. Lin et al. [24] proposed an IoT-based sprinkler and fertilization system with short- and long-term preparedness. The system uses integer linear programming to allocate limited resources across several crops to optimize the economy as well as the environment. These trials show that the optimization approach helps precise farming manage irrigation and fertilizer sustainably. Gupta et al. [25] developed a technique for cell-phones and OBD systems. Bi-level optimization is used in this light-weight and effective AI technique. When optimizing artificial neural networks (ANNs), it handles binary input characteristics, integer neurons that are concealed and actual relationship weights well. A genetic

algorithm (GA) performs evolutionary optimization on binary characteristics and numerical hidden neurons at Level-I. The dual-level strategy optimizes and improves technology flexibility to edge device factors.

Rezk et al. [26] have introduced an intelligent methodology that combines the wrapper feature selection approach with the PART classification technique for assessing crop productivity. The Wrapper technique is applied to scrutinize environmental indicators' collected data, identifying the most influential factors in addressing drought and crop production issues. PART algorithm is used to construct the predictor for drought and crop productivity. The WPART method achieves exceptional accuracy, surpassing existing standard algorithms. It reaches up to 92.51 %, 96.77 %, 98.04 %, 96.12 %, and 98.15 % for the five datasets related to famine cataloging then yield efficiency, correspondingly. Akhter et al. [27] have introduced an economical and energy-efficient planar inter digital phosphate sensor designed for smart agriculture. To validate the experimental findings, standard UV Spectrometry is employed, enhancing the reliability of the sensor. This innovative system allows for the assessment of water quality from any location, with the ability to seek expert opinions remotely, thereby enhancing the accessibility and efficiency of phosphate detection in agricultural settings. Anand et al. [28] presented AgriSegNet, an architecture for deep aerial segmentation based on semantics that is designed for pattern detection in agriculture utilizing UAV-obtained aerial pictures. Agri-SegNet makes use of two separate picture scales that are inputted into the network. While the backbone retrieves data from the DeepLabV3+ model, the attention head uses weighted ratio to combine features from different scales. Roy et al. [29] designed AgriSens, connected to the internet of variable irrigation scheduling system for irrigated agriculture areas. AgriSens uses IoT to provide real-time, automated, changing, and remotely irrigation services for different agricultural growth stages. Results show that AgriSens improves crop output by 10.21 % over manual watering. Even after 500 hours of uninterrupted operation, the system achieves 94 % reliability and 2.5 times network lifespan. Atalla et al. [30] assessed WSN performance using 6LowPAN and RPL routing protocol. The RPL technique was evaluated in two agricultural settings and modeled using COOJA.

The intelligent decision-making framework for the farming industry, developed by Mekala et al. [31], includes a process for selecting sensor and an all-encompassing measuring index called THAM. To find the best node specification for the field, it uses the thermal proportion, the NPK fertilizers regulating approach, and the agricultural science functions. The (t, n) bulgeconditiondirectorydescribes the ideal amount of devices needed for effective arena monitoring. The thermal proportion evaluates the growth rate by considering soil temperature and moisture levels. The agronomy function, which factors in aquatic pH level and SO₂ attentiveness in the air, measures the makingharvestamount of the field. The model enhances forecastpresentation, improving the detection of abnormal conditions by 75 %. Additionally, it reduces the generation of irrelevant data and minimizes resource loss, making valuable tool for optimizes agricultural decision-making processes. Data from many sources may be seamlessly integrated in IoT-enabled precision agriculture.

This integrated method gives a complete picture of the agriculture environment, aiding decision-making [21]. Advanced analytics and modeling are needed to anticipate weather, crop, and soil conditions. Farmers may make data-driven crop management decisions using IoT devices' vast datasets and powerful machine learning and analytics algorithms to forecast future trends and enhance farming operations [22–24]. Proper assignment, calibration, and maintenance of sensor nodes across the field for full coverage are difficult [25]. However, intelligent placement and design of IoT nodes for sensors can improve coverage, and frequent maintenance ensures data accuracy [26]. Communication challenges between IoT devices and the central monitoring system may arise in remote or large agricultural fields. Data security and privacy concerns arise due to the sensitive nature of agricultural data. IoT-enabled precision agriculture addresses these

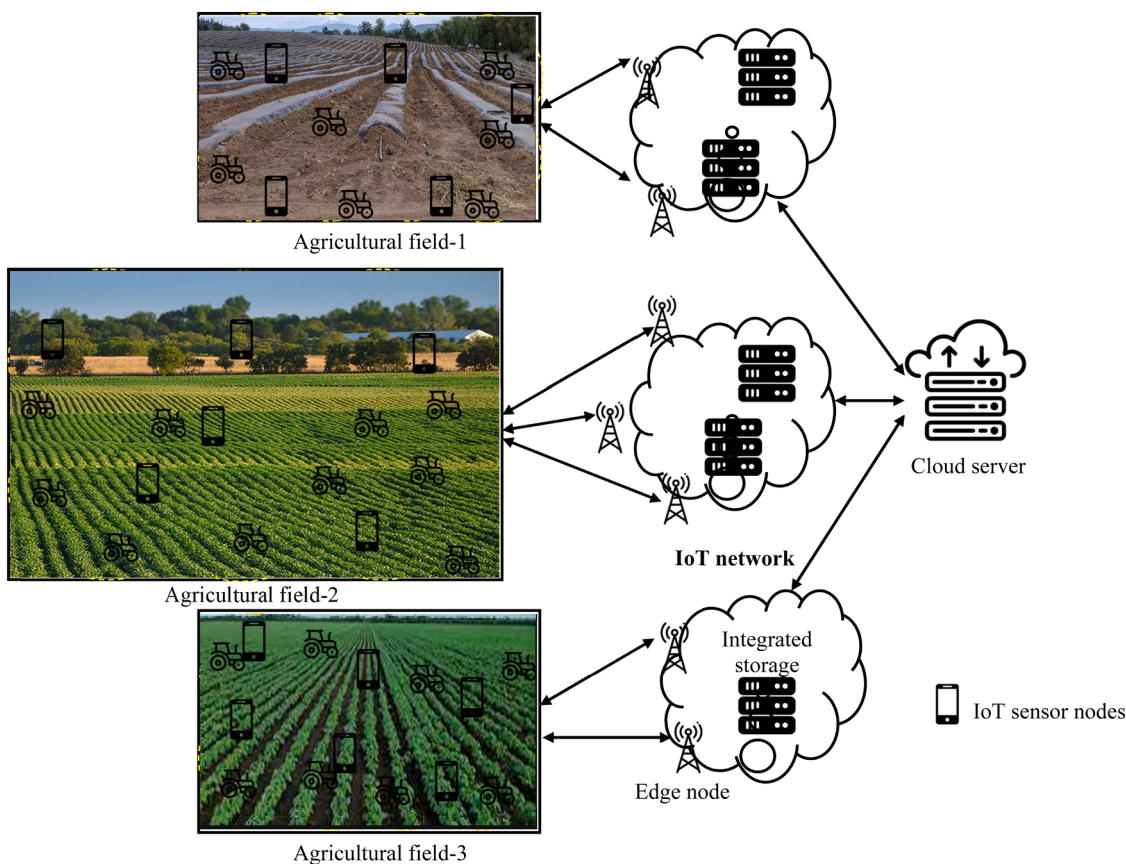


Fig. 1. Network view of proposed smart optimal prediction model for sensors using IoT-enabled precision agriculture.

concerns by implementing robust security measures, including encryption and secure communication protocols [27,28]. Compliance with data protection regulations ensures the privacy of farmers and their operations. The cost of implementing IoT infrastructure is a barrier for some farmers. However, over time, as technology matures and becomes more widespread, the cost of IoT devices and solutions is expected to decrease [29]. Government incentives and support programs can further assist farmers in adopting precision agriculture technologies. While IoT-enabled agriculture offers solutions to challenges, careful planning, maintenance, and addressing potential issues related to node deployments and communication are essential for successful implementation [30,31]. To address those problems, we presented a smart optimal prediction model for IoT-enabled precision agriculture. The key objectives of proposed work are given as follows.

1. Explore communication technologies to address challenges in remote or large fields, improving data transmission reliability.
2. Improve the accuracy and reliability of IoT sensor data for weather, field conditions, and soil parameters.
3. Create sophisticated predictive analytics models and algorithms for precise forecasting of weather changes, crop growth, and soil conditions.
4. Investigate optimal strategies for deploying IoT sensor nodes in agricultural fields, considering coverage, calibration, and maintenance.

3. Structure of information

In the proposed model, we aim to develop an intelligent and optimal prediction system for sensors within the context of IoT-enabled precision agriculture. Our focus encompasses three key components. Firstly, we concentrate on optimizing the THAM index. These systems typically

analyze and categorize results grounded on thermal capacities ($t.\max$) throughout the seasonal period. Specifically, three levels are considered [31]:

- Comfort level: ($t.\max \geq 28^{\circ}\text{C}$)
- Uncomfortable conditions: ($t.\max \geq 35^{\circ}\text{C}$)
- Highly uncomfortable conditions: ($t.\max \geq 40^{\circ}\text{C}$)

Moisture, represented by water vapor pressure (pulmonary stress index), is also a crucial factor. Relative humidity measurements are categorized into three levels [31]:

- Appropriate comfort level: $\approx 50\%$ (30–70 %)
- Dry conditions: Below 30 %
- Humid conditions: Over 70–80 %

Due to air pollution, the latter two the humidity levels may raise heart and lung disease risk in people. High humidity might also affect crop development. The first difficulty is inappropriate sensor deployment over agricultural areas and sensor selection that generates duplicate data. Poor soil health and fertilizer for agricultural crops wastes environmental resources. As indicated in Fig. 1, global agricultural monitoring is needed. IoT applications in smart farming, transportation, and healthcare generate too much data for measurement analysis. The goal is to create a novel field cover making choices system that boosts crop yields and IoT agricultural application performance. Environmental factors must be accurately measured to avoid useless data. This aim requires a sequence of successive steps. Subdivide the farming area $A = \{a_1, a_2, a_3, \dots, a_x\}$ into $L \times L$ square foot sub-areas. For better communication and information coverage, sensors are arranged by radius range R . To establish an efficient smart farming observing systems, a diverse set of effort strictures must be incorporated,

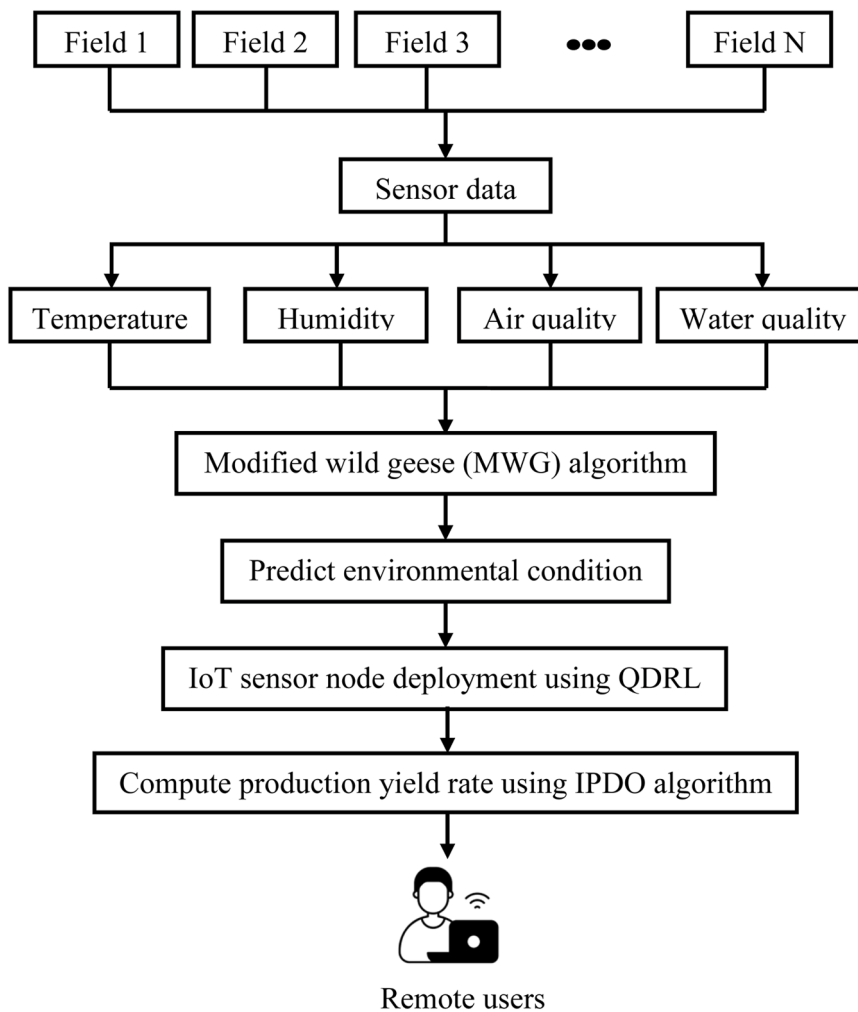


Fig. 2. Overview of smart optimal prediction model for sensors.

encompassing dirt factors like formation, electrical conductivity (EC), pH, thermal, and moisture, alongside ecological factors such as carbon monoxide (CO), carbon dioxide (CO₂), and injurious smokes like nitrous acid and ammonia. Fig. 2 provides an overview of the proposed smart optimal prediction model for sensors within IoT-enabled precision agriculture. Data streams, including thermal, dirt dampness, aquatic level, pH, and air CO and CO₂ concentrations, are directed to the sensor cloud for comprehensive assessment and precise deciding. The data fusion is used to eliminate redundant and noisy data, refining the dataset for subsequent processing. The core of the system lies in the third step, where decision-making occurs based on predefined threshold data. Statistical analyses are employed to classify these decisions, identifying different condition levels. The outcomes of this analysis serve as input for the final step, where decisions are distributed to end users through SMS or emails. This comprehensive approach ensures effective data processing, decision-making, and timely communication, ultimately enhancing the control and efficiency of the smart agriculture monitoring system, enabling remote management of the field area.

4. Proposed methodology

4.1. THAM index optimization

Our THAM index optimization method uses the altered wild geese (MWG) algorithm. Highly accurate environmental prediction is possible with it. THAM index is a critical indicator for precision agriculture since it measures environmental well-being. Adaptable and effective in

managing complicated environmental data, MWG algorithm is used. The algorithm is fed temperature, humidity, and air and water quality readings to start this optimization process. Inspired by wild geese, the MWG algorithm adapts and collaborates to improve its predictions. As the MWG algorithm continues, it refines its forecasts to account for the complex relationship between temperature, humidity, and air and water quality. This recurrent refining procedure lets the system respond to dynamic changes in the environment for accurate prediction. MWG algorithm to THAM index optimization may improve precision agricultural environmental monitoring systems. By precisely anticipating and optimizing these environmental characteristics, we can improve decision-making and agricultural output and resource use. This customized optimization technique supports IoT-enabled precise agriculture, where data-driven conclusions are essential for sustainable and effective farming. The MWG method for multidimensional problems in optimization is based on the life cycle of wild geese, which includes their regular and synchronized group movement, development, evolution, and mortality. Velocity and displacement equations according to the coordinated velocity of the geese are given as follows.

$$\begin{aligned}
 V_{h,c}^{iter+1} = & \left(R_{1,c} \times V_{h,c}^{iter} + R_{2,c} \times \left(V_{1+h,c}^{iter} - V_{h-1,c}^{iter} \right) \right) \\
 & + R_{3,c} \times \left(x_{h,c}^{iter} - p_{h-1,c}^{iter} \right) + R_{4,c} \times \left(x_{h+1,c}^{iter} - p_{h,c}^{iter} \right) \\
 & + R_{5,c} \times \left(x_{h+2,c}^{iter} - p_{h+1,c}^{iter} \right) + R_{6,c} \times \left(x_{h-1,c}^{iter} - p_{h+2,c}^{iter} \right)
 \end{aligned} \quad (1)$$

where $p_{h,c}$, $x_{h,c}$, and $V_{h,c}$ are the c-th measurement of the present location,

Algorithm 1

THAM index optimization using MWG.

Input: Sensor data, maximum iteration and termination condition
Output: THAM index optimization

1. Initialize the random population
2. The synchronized speed of the geese is $V_{h,c}^{iter+1}$
3. If $i=0, j=1$
4. While Do
5. Define the movement of all members as an ordered series
 $p_{h,c}^V = x_{h,c}^{iter} + R_{1,c} \times ((j_c^{iter} + x_{h+1,c}^{iter} - 2 \times x_{h,c}^{iter}) + V_{h,c}^{iter+1})$
6. Define the optimal function $p_{h,c}^{iter+1} = \begin{cases} p_{h,c}^V & \text{if } R_{11,c} \leq cr \\ p_{h,c}^z & \text{otherwise} \end{cases}$
7. Maximize $r_t = F(R, b)$
8. Compute nonlinear reliability-redundancy constrained optimization
 $F(p) = \sum_{s=0}^{100} (q(s) - q_0(s))^2$
9. End

the finest location, and the present speed of the h-th wild goose, correspondingly.

$$p_{h,c}^V = x_{h,c}^{iter} + R_{1,c} \times ((j_c^{iter} + x_{h+1,c}^{iter} - 2 \times x_{h,c}^{iter}) + V_{h,c}^{iter+1}) \quad (2)$$

where j_c is the universal top place among all associates. This stage is demonstrated in such a method that the h-th wild goose changes to its open associate, i.e. the $(h+1)$ -th goose ($x_{h+1}^{iter} - x_h^{iter}$). In alternative term, the h-th goose attempts to grasp the $(h+1)$ -th goose ($x_{h+1}^{iter} - x_h^{iter}$). The purpose for searching and walking for diet by the wild goose p_h^z is as follows:

$$p_{h,c}^z = x_{h,c}^{iter} + R_{9,c} \times R_{10,c} (x_{h+1,c}^{iter} - x_{h,c}^{iter}) \quad (3)$$

Alternative phase of wild geese's lifecycle is evolution and reproduction. In this paper, its demonstrating is achieved so that a mixture amid relocation reckoning (p_h^V) and walking and exploration for food calculation (p_h^z) is used. The Cr worth for the projected WGA algorithm is 0.5 in total imitation.

$$p_{h,c}^{iter+1} = \begin{cases} p_{h,c}^V & \text{if } R_{11,c} \leq cr \\ p_{h,c}^z & \text{otherwise} \end{cases} \quad (4)$$

The expiry stage is active in directive to poised algorithm performance for all test functions. In this phase, the algorithm starts with the maximum population number $Bx^{initial}$ and during the algorithm iterations, the weaker members will be removed from the population and the population scope will cut linearly grasps its concluding value Bx^{Final} in the final iteration.

$$Bx = Round \left(\begin{array}{c} Bx^{initial} \\ -((Bx^{initial} - Bx^{Final}) * \left(\frac{fes}{fes_{Max}} \right)) \end{array} \right) \quad (5)$$

where fes and fes_{Max} are the amount of purpose assessments and its extreme. The sound surfs for t definite in variety of 1–100 are as trails.

$$q(s) = p_1 \sin(p_2 s\theta + p_3 \sin(p_4 s\theta + p_5 \sin(p_6 s\theta))) \quad (6)$$

$$q_0(s) = 1.0 * \sin(0.5s\theta + 0.5 * \sin(4.8s\theta + 2.0 * \sin(4.9s\theta))) \quad (7)$$

where $\theta = 2\pi/100$. Taken as a whole, the goal or variable of the optimization issue is squared errors between $q(s)$ and $q_0(s)$ with optimal value $F(p) = 0$ as follows:

$$F(p) = \sum_{s=0}^{100} (q(s) - q_0(s))^2 \quad (8)$$

Improving durability by making the most of the component reliability vectors is the primary goal of complex durability-redundancy

restricted optimization issues $R = (R_1, R_2, \dots, R_a)$ and redundancy assignment vector $b = (b_1, b_2, \dots, b_a)$ for subsystems of the system.

$$\text{Maximize } r_t = F(R, b) \quad (9)$$

$$\text{subject to } j(R, b) \leq L, \quad 0 \leq R_c \leq 1, \quad n_c \in W^+, \quad 0 \leq c \leq a \quad (10)$$

where W^+ is the set of optimistic numerals, r_t signifies the dependability of numerous schemes, $f(\cdot)$ and $j(\cdot)$ signify for the impartial and restraint roles of optimal problematic for the total parallel-series schemes, [algorithm 1](#) describes the working process of the THAM index optimization using MWG.

4.2. Sensor node deployment

Transitioning from THAM index optimization, our next focal point is the strategic deployment of IoT sensor nodes, and we employ quantum deep reinforcement learning (QDRL) to ascertain the optimal number of sensors essential for achieving efficient coverage in the designated agricultural field. This deployment strategy not only aims to enhance coverage but also works towards improving communication within the precision agriculture system. The use of QDRL in sensor node deployment is cutting-edge. Quantum computing along with deep reinforcement learning underpin QDRL's advanced decision-making framework in dynamic and complicated contexts. QDRL specializes when choosing the best placements and number of sensors for agricultural field coverage. QDRL uses quantum concepts to investigate several options concurrently, improving sensor node placement decisions. Quantum parallelism effectively searches the enormous solution space to find the best configuration for coverage and redundancy. QDRL considers agricultural field topography, environmental factors, and prospective areas of interest throughout installation. By using QDRL in sensor node deployment process, we aim to revolutionize precision agriculture by achieving not optimal coverage but also by facilitating enhanced communication between deployed sensors. The contribution to QDBNs is statistics after the situation, i.e. $\{\eta_1, \eta_2, \eta_h, \dots, \eta_{BHB}\}$; where N IN is the number of dimensions of the input data. The results of DBNs are the predicted states for the ecological states in next iteration, i.e., $\{t'_1, t'_2, t'_h, \dots, t'_{B_{out}}\}$; wherever t' is the amount of control procedure in the atmosphere. QDRL-based agent control strategies from the action set by updating the Y-value matrix and the X-value matrix as follows:

$$Y_{rl}(T, m) = Y_{rl}(t, m) + \alpha_{rl} \max_{m \in M} Y_{rl}(t', m) - Y_{rl}(t, m) \quad (11)$$

$$X_{rl}(t', m) = \begin{cases} X_{rl}(t, m) - \beta_{rl} (1 - X_{rl}(t, m)) & \text{if } m' = m \\ X_{rl}(t, m) - (1 - \beta_{rl}) & \text{if } X_{rl} \neq a \end{cases} \quad (12)$$

where α_{rl}, β_{rl} , and γ_{rl} are learning, improvement, and discount coefficient, respectively. In general, all these coefficients α_{rl}, β_{rl} , and γ_{rl} are built in series, $\alpha_{rl}, \beta_{rl}, \gamma_{rl} \in (0, 1)$; t , t' and m are current state, predicted next state and action state, respectively. An x-value medium of support knowledge can score the likelihood of each action in each state.

$$r_{rl}(t, t', m) = \begin{cases} 10, & |E_{error}| \leq 0.005 \\ -|E_{error}|^2, & |E_{error}| > 0.005 \end{cases} \quad (13)$$

If the absolute control error E_{error} is less than a built-in threshold (0.005) the reward value can be set to a positive number. The limited Boltzmann machine potential of QDRL can be definite as follows.

$$e(V, H|\theta) = - \sum_{h=1}^{B_{layer}} c_h V_h - \sum_{g=1}^{B_{Hidden}} c_g V_g - \sum_{h=1}^{B_{layer}} \sum_{g=1}^{B_{Hidden}} V_h Z_{hg} i_g \quad (14)$$

where Z_{hg} is the load from nerve units to others. The training process of QDRL can update the mass of noticeable components, base counterbalance i and V_h base counterbalance c_g of concealed units i_g . The probability distribution of (V, H) can be calculated as:

Algorithm 2

Sensor node deployment using QDRL.

-
- Input: Environmental condition, number of sensor nodes, training and testing set
Output: Sensor node deployment
1. Initialize the random population
 2. The ARL by updating the Y-value matrix and the X-value matrix
$$Y_{rl}(T', m) = Y_{rl}(t, m) + \alpha_{rl}(t, t', m) + \gamma_{rl} \text{Max}_{m \in M} Y_{rl}(t', m) - Y_{rl}(t, m))$$
 3. If i=0, j=1
 4. Compute QDRL reward value $r_{rl}(t, t', m) = \begin{cases} 10, & |E_{error}| \leq 0.005 \\ -|E_{error}|^2, & |E_{error}| > 0.005 \end{cases}$
 5. Define h-th solution of QDRL $m'_{hOUT} = m_K + \frac{m_{(K+1)} - m_{(K-1)}}{2} \left(y_h(m) - \frac{1}{2} \right)$
 6. Compute fitness function $y_h(m) = |\vec{m}_t^{B_M}\rangle = \sum_{m=0..00}^{\overbrace{11\dots1}^{N_y}} D_m |m\rangle$
 7. Update the output value
 8. End
-

$$X_{cl}(V, H|\theta) = \frac{E^{-e(V, H|\theta)}}{\sum_{V,i} E^{-e(V, H|\theta)}} \quad (15)$$

where V, H, and θ denote visible unit, hidden unit, and sample vectors, respectively. The active functions of the projected likelihood of concealed and noticeable units are assumed as follows:

$$X_{cl}(i_g = 1 | V, \theta) = \frac{1}{1 + E^{(-(n_g + \sum_h V_h Z_{hg}))}} \quad (16)$$

$$X_{cl}(V_h = 1 | i, \theta) = \frac{1}{1 + E^{(-\left(c_h + \sum_g i_g Z_{hg}\right))}} \quad (17)$$

A selfish empowered learning technique for choosing an action yields the best local answer. The QDRL uses quantum procedures to prevent the optimum localized answer. The QDRL h-th answer is determined as following.

$$m'_{hOUT} = m_K + \frac{m_{(K+1)} - m_{(K-1)}}{2} \left(y_h(m) - \frac{1}{2} \right) \quad (18)$$

where together $m_{(K+1)}$ and $m_{(K-1)}$ are the activities of deed set M; m_K is the elected act from action set M by the strengthening knowledge of the QDRL; and $y_h(m)$ is the output chance, $0 \leq y_h(m) \leq 1$, which is designed as follows.

$$y_h(m) = |\vec{m}_t^{B_M}\rangle = \sum_{m=0..00}^{\overbrace{11\dots1}^{N_y}} D_m |m\rangle \quad (19)$$

Actions $|D_m|^2$ mean the possibility of action $|\vec{m}_t^{B_M}\rangle$ by the number of quantum bits. This quantum process of QDRL is different from quantum reinforcement learning. It has many quantum states and many quantum functions. The [algorithm 2](#) describes the working steps of proposed sensor node deployment using QDRL.

4.3. Production yield rate computation

In the pursuit of comprehensive precision agriculture, our attention now turns to the crucial task of computing the production yield rate. This involves a multifaceted approach, taking into consideration various attributes including fertilizer regulatory measures, temperature quotient, and agronomy. Advanced optimization techniques like the improved prairie dog optimization (IPDO) algorithm optimize these parameters to increase production yield rate computation efficiency. The IPDO method is used to optimize production yield-affecting factors. This program applies prairie dog colony collaboration and adaptability to agricultural optimization. First, examine fertilizer regulations. The IPDO algorithm optimizes fertilizer delivery depending on soil condition, crop need, and regulatory guidelines via incremental and reactive

procedures. This makes fertilizer usage effective and sustainable, supporting crop development according to agricultural regulations. The IPDO algorithm carefully controls the ambient temperature quotient, another important factor. It optimizes agricultural techniques to reduce the negative impact of severe temperatures on crop output by considering crop-specific ideal temperature ranges. The IPDO algorithm optimizes the care of the soil, rotation of crops, and methods of cultivation, including agronomy. IPDO's continuous and adaptive nature allows for continual attribute optimization refining. Populations of XC act as search agents, and each XC is represented by a vector in the D-dimensional space. Each PD of a coterie is portion of one of n coteries. A course can follow all X to a positive coterie because the X acts as a cluster or collective. The medium underneath signifies the status of all coterie (DS) in the group.

$$DS = \begin{bmatrix} DS_{1,1} & DS_{1,2} & \dots & DS_{1,c-1} & DS_{1,c} \\ DS_{2,1} & DS_{2,2} & \dots & DS_{2,c-1} & DS_{2,c} \\ \vdots & \vdots & DS_{h,g} & \vdots & \vdots \\ DS_{a,1} & DS_{a,2} & \dots & DS_{a,c-1} & DS_{a,c} \end{bmatrix} \quad (20)$$

Here, $DS_{h,g}$ the h-th coterie represents the g-th dimension.

$$XC = \begin{bmatrix} XC_{1,1} & XC_{1,2} & \dots & XC_{1,c-1} & XC_{1,c} \\ XC_{2,1} & XC_{2,2} & \dots & XC_{2,c-1} & XC_{2,c} \\ \vdots & \vdots & XC_{h,g} & \vdots & \vdots \\ XC_{b,1} & XC_{b,2} & \dots & XC_{b,c-1} & XC_{b,c} \end{bmatrix} \quad (21)$$

where $XC_{h,g}$ represents the h-th prairie dog in the g-th dimension of the coterie. Conferring to the calculations beneath, a varying supply is used to allocate all DS and XC spot.

$$DS_{h,g} = U(0, 1) * (UN_g - LN_g) + LN_g \quad (22)$$

$$XC_{h,g} = U(0, 1) * (un_g - ln_g) + ln_g \quad (23)$$

In this case $un_j = \frac{UN_g}{a}$, $ln_j = \frac{LN_g}{a}$, $U(0, 1)$, accidental amount is distributed amid 0 and 1. UN_g and LN_g are the lower and upper limits of g-th measurement of the optimized problem.

$$F(XC) = \begin{bmatrix} F_1 \left[\begin{matrix} XC_{1,1} & XC_{1,2} & \dots & XC_{1,c-1} & XC_{1,c} \end{matrix} \right] \\ F_2 \left[\begin{matrix} XC_{2,1} & XC_{2,2} & \dots & XC_{2,c-1} & XC_{2,c} \end{matrix} \right] \\ \vdots & \ddots & \vdots & \vdots & \vdots \\ F_b \left[\begin{matrix} XC_{b,1} & XC_{b,2} & \dots & XC_{b,c-1} & XC_{b,c} \end{matrix} \right] \end{bmatrix} \quad (24)$$

The next three are of great value for creating burrows that help them escape from predators. The maximum number of iterations is divided into four parts: the first two are for exploration and the last two are for exploitation.

$$iter < \frac{Max_{iter}}{4} \text{ and } \frac{Max_{iter}}{4} \leq iter < \frac{Max_{iter}}{2} \quad (25)$$

whilst the two approaches for mistreatment are reliant on

$$\frac{Max_{iter}}{2} \leq iter \leq 3 \frac{Max_{iter}}{4} \text{ and } 3 \frac{Max_{iter}}{4} \leq iter \leq Max_{iter} \quad (26)$$

During the exploration phase, the coterie's initial strategy is to find new food sources in the chamber for members.

$$XC_{h+1,g+1} = Jbest_{hg} - EDbest_{hg} \times \rho - cpd_{hg} \times levy(b) \forall iter < \frac{Max_{iter}}{4} \quad (27)$$

$$XC_{h+1,g+1} = Jbest_{hg} \times RXC \times CT \times levy(b) \forall iter \frac{Max_{iter}}{4} \leq iter < \frac{Max_{iter}}{2} \quad (28)$$

The results are $EDbest_{h,d}$ evaluated for most effective solution currently available globally and $Jbest_{hg}$ represent best solution available globally. Lévy distribution ($Lévy(p)$), facilitates the optimal and efficient search of the problem space.

Algorithm 3

Production yield rate computation using IPDO.

Input: Fertilizer regulatory, temperature quotient, and agronomy
 Output: Production yield rate

1. Initialize the random population
2. The unvarying circulation is cast off to allocate all DS then XC site.
 $DS_{hg} = U(0, 1) * (UN_g - LN_g) + LN_g$ and $XC_{hg} = U(0, 1) * (un_g - ln_g) + ln_g$
3. If $i=0, j=1$
4. While Do
5. Define mistreatment of fitness computation
 $\frac{Max_{iter}}{2} \leq iter \leq 3 \frac{Max_{iter}}{4}$ and $3 \frac{Max_{iter}}{4} \leq iter \leq Max_{iter}$
6. Compute optimal fitness
 $XC_{h+1,g+1} = Jbest_{hg} - EDbest_{hg} \times \rho - cpd_{hg} \times levy(b) \forall iter < \frac{Max_{iter}}{4}$
7. else
8. Compute the marauder result $Xe = 1.5 \times \left(1 - \frac{iter}{Max_{iter}}\right)^{\left(\frac{2}{Max_{iter}}\right)}$
9. End if
10. Update the final value
11. End

$$EDbest_{h,d} = Jbest_{hg} \times \Delta + \frac{XC_{hg} \times mean(XC_{b,a})}{Hbest_{hg} \times (UN_g - LN_g) + \Delta} \quad (29)$$

$$cpd_{hg} = \frac{Jbest_{hg} - RXC_{hg}}{Jbest_{hg} + \Delta} \quad (30)$$

$$CT = 1.5 \times R \times \left(1 - \frac{iter}{Max_{iter}}\right)^{\left(\frac{2}{Max_{iter}}\right)} \quad (31)$$

where Δ is a random number representing the imbalance between CT and R, introducing a random property to stabilize the probes and taking the value -1 or 1 based on the present repetition. r adds a random stuff to guarantee examination and receipts the value -1 or 1 contingent on the existing repetition. s

$$\frac{Max_{iter}}{2} \leq iter \leq 3 \frac{Max_{iter}}{4} \text{ and } 3 \frac{Max_{iter}}{4} \leq iter \leq Max_{iter} \quad (32)$$

$$XC_{h+1,g+1} = Jbest_{hg} - EDbest_{hg} \times \epsilon - cpd_{hg} \times rand \sqrt{\frac{Max_{iter}}{2}} \leq iter \\ < 3 \frac{Max_{iter}}{4} \quad (33)$$

$$XC_{h+1,g+1} = Jbest_{hg} - Xe \times rand \sqrt{3 \frac{Max_{iter}}{2}} \leq iter < Max_{iter} \quad (34)$$

Analyzes the $EDbest_{hg}$ impact of the record effective universal key- $Jbest_{hg}$ is used to compute the optimal solution. Max_{iter} is the present repetition and $iter$ is the amount of repetitions. ϵ is a small value representing food quality, which is cpd_{hg} combined effect of each XC in the group, $rand$ is a accidental sum among 0 and 1, and Xe is the marauder result.

$$Xe = 1.5 \times \left(1 - \frac{iter}{Max_{iter}}\right)^{\left(\frac{2}{Max_{iter}}\right)} \quad (35)$$

The [algorithm 3](#) describes the working process of production yield rate computation using IPDO.

5. Results and discussion

Our model findings and IoT-enabled precise agricultural model comparisons are presented in this section. The MWG-QDRL-IPDO variant was tested on Lenovo PCs with Intel(R) Core i5-2557M 1.70GHz processors and 4GB RAM. Network simulators and MATLAB R2015 were used for modeling. The bureau of meteorology, LSM, and Phenonet provided sensor data. Our tree farm tests used an IoT infrastructure with 36 sensor nodes, every symbolizing a tree equipped with relay nodes. The nodes were strategically positioned on a grid in 25 m \times 25 m, 50 m \times 50 m, 75 m \times 75 m, and 100 m \times 100 m squared sectors. [Fig. 3](#) depicts our simulation experiment. Data collection and transmission were centralized at the sink node in the simulation region. This arrangement let us assess network performance and examine how the number of nodes and area coverage affect system performance.



[Fig. 3](#). Simulation setup of our proposed MWG-QDRL-IPDO model for precision agriculture.

Table 1

Results comparison for node deployment models with different sensor searching range and temperature sensors.

Model	Sensor search rate (%)									
	20 Number of selected sensors	40	60	80	100	20 Accuracy (%)	40	60	80	100
R-model	15	18	22	23	25	60.23	62.35	63.26	64.23	66.95
O-model	14	17	21	22	24	68.92	71.04	71.95	72.92	75.64
(t, n)-model	13	16	20	21	23	77.61	79.73	80.64	81.61	84.33
MWG-QDRL-IPDO model	12	15	19	20	22	88.30	90.42	91.33	92.30	95.02
Processing time (ms)										
R-model	42,000	42,500	43,000	43,500	44,000	62.29	64.41	65.32	66.29	69.01
O-model	32,000	32,500	33,000	33,500	34,000	70.98	73.10	74.01	74.98	77.70
(t, n)-model	22,000	22,500	23,000	23,500	24,000	79.66	81.79	82.69	83.66	86.39
MWG-QDRL-IPDO model	12,000	12,500	13,000	13,500	14,000	90.358	92.47	93.38	94.35	97.07

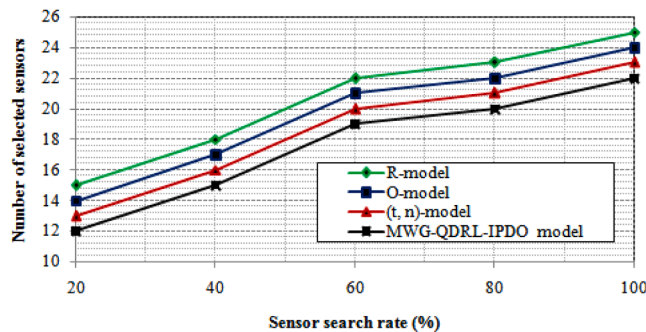


Fig. 4. Number of selected sensors comparison for temperature sensor case.

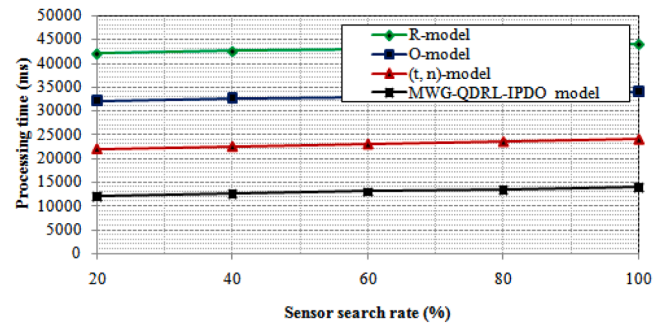


Fig. 6. Processing time comparison for temperature sensor case.

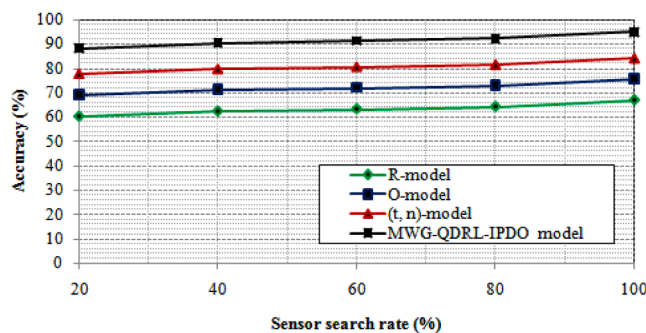


Fig. 5. Accuracy comparison for temperature sensor case.

5.1. Comparative analysis with respect to node deployment

Table 1 presents a concise comparison of results for node deployment models with varied sensor searching ranges and temperature sensors. In Fig. 4, a comprehensive comparison of the number of selected sensors for the temperature sensor case is presented among different models—R-model, O-model, (t, n)-model, and our proposed MWG-QDRL-IPDO model. For the R-model, as the sensor search rate increases, the number of selected sensors follows suit, with a percentage-wise increase observed at each step. At a 20 % search rate, 15 sensors are selected, rising to 25 sensors at a 100 % search rate. Similarly, the O-model demonstrates an increase in the number of selected sensors with an ascending sensor search rate, showing increments from 14 sensors at 20 % to 24 sensors at 100 %. The (t, n)-model exhibits a comparable trend, illustrating an increase in selected sensors from 13 at 20 % to 23 at 100 % search rate. In contrast, our MWG-QDRL-IPDO model outperforms the existing models with respect to efficiency. Despite the ascending sensor search rate, the number of selected sensors shows a decrease, ranging from 12 sensors at 20 % to 22 sensors at 100 %. In Fig. 5, we present a detailed comparison of accuracy for the temperature sensor case across

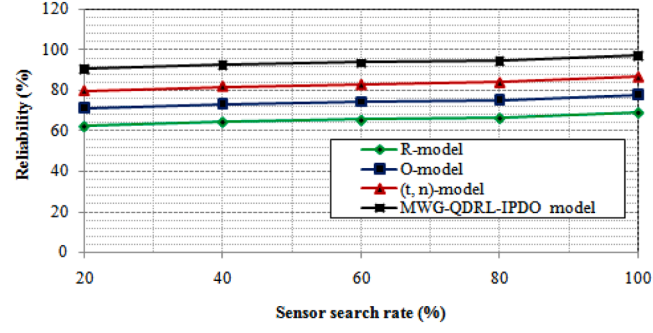


Fig. 7. Reliability comparison for temperature sensor case.

different models. For the R-model, an incremental trend is observed in accuracy as the sensor search rate increases, ranging from 60.23 % at 20 % search rate to 66.95 % at 100 %, indicating an increase. Similarly, the O-model exhibits a consistent increase in accuracy from 68.92 % at 20 % to 75.64 % at 100 %, representing an increase. The (t, n)-model follows suit with an increase in accuracy, ranging from 77.61 % at 20 % to 84.33 % at 100 % search rate. In contrast, our MWG-QDRL-IPDO model shows remarkable accuracy, with accuracy experiencing an increase. The accuracy ranges from 88.3 % at 20 % to an impressive 95.02 % at 100 % search rate.

In Fig. 6, a comprehensive comparison of processing time for the temperature sensor case is depicted across different models. For the R-model, there is an increase in processing time as the sensor search rate escalates, ranging from 42,000 milliseconds at 20 % search rate to 44,000 milliseconds at 100 %, indicating an improvement. Similarly, O-model exhibits an incremental trend in processing time from 32,000 ms at 20 % to 34,000 ms at 100 %, representing an improvement. The (t, n)-model follows suit with an improvement in processing time, ranging from 22,000 ms at 20 % to 24,000 ms at 100 % search rate. In contrast, our MWG-QDRL-IPDO model showcases a more efficient and optimized processing time. Despite the ascending sensor search rate, there is an

Table 2

Results comparison for node deployment models with different sensor searching range and Soil EC sensor case.

Model	Sensor search rate (%)									
	20 Number of selected sensors	40	60	80	100	20	40	60	80	100
R-model	9	11	16	19	22	75.89	77.90	79.05	81.28	83.52
O-model	11	13	18	21	24	79.58	81.59	82.74	84.97	87.21
(t, n)-model	13	15	20	23	26	83.27	85.27	86.43	88.66	90.90
MWG-QDRL-IPDO model	15	17	22	25	28	86.96	88.96	90.12	92.35	94.58
Processing time (ms)										
R-model	43,500	45,000	45,500	46,500	47,500	63.34	65.46	66.37	67.34	70.06
O-model	33,500	35,000	35,500	36,500	37,500	72.03	74.15	75.06	76.03	78.75
(t, n)-model	23,500	25,000	25,500	26,500	27,500	80.72	82.84	83.75	84.72	87.44
MWG-QDRL-IPDO model	13,500	15,000	15,500	16,500	17,500	91.41	93.53	94.44	95.41	98.13

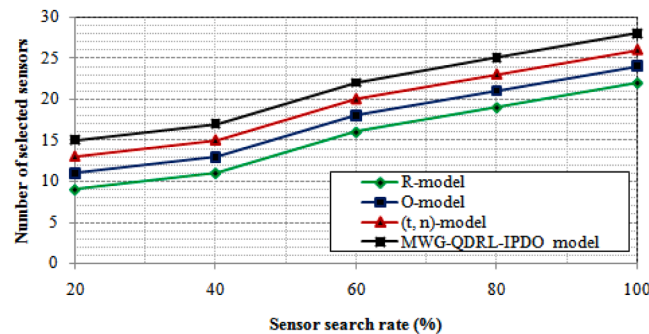


Fig. 8. Number of selected sensors comparison for Soil EC sensor case.

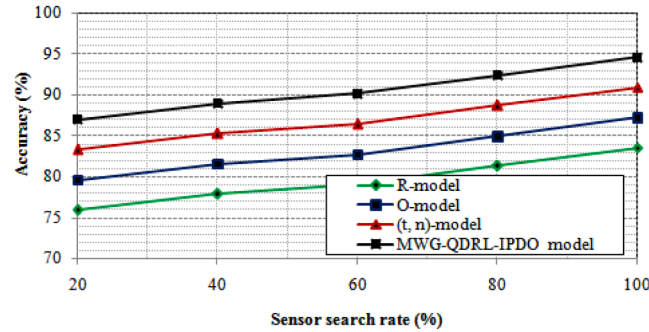


Fig. 9. Accuracy comparison for Soil EC sensor case.

improvement in processing time, ranging from 12,000 ms at 20 % to 14,000 ms at 100 %. This underscores the efficiency of the MWG-QDRL-IPDO model in optimizing processing time for temperature monitoring, showcasing a more resource-efficient approach compared to the existing models.

In Fig. 7, we present a detailed comparison of reliability for the temperature sensor case among different models. For the R-model, there is a consistent increase in reliability as the sensor search rate escalates, ranging from 62.29 % at 20 % search rate to 69.01 % at 100 %, indicating an improvement. Similarly, the O-model exhibits an incremental trend in reliability from 70.98 % at 20 % to 77.70 % at 100 %, representing an improvement. The (t, n)-model follows suit with an improvement in reliability, ranging from 79.66 % at 20 % to 86.39 % at 100 % search rate. In contrast, our MWG-QDRL-IPDO model shows an improvement in reliability. The reliability ranges from 90.35 % at 20 % to an impressive 97.07 % at 100 % search rate. This emphasizes the superior reliability of the MWG-QDRL-IPDO model for temperature monitoring compared to existing models.

Table 2 presents a concise comparison of results for node deployment models with varied sensor searching ranges and Soil EC sensors. In Fig. 8,

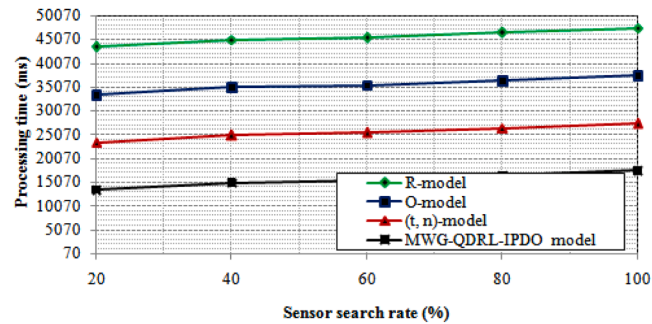


Fig. 10. Processing time comparison for Soil EC sensor case.

a detailed comparison of the number of selected sensors for the Soil EC sensor case is presented among different models. For the R-model, there is an increase in the number of selected sensors as the sensor search rate escalates, ranging from 9 sensors at 20 % search rate to 22 sensors at 100 %, indicating an improvement. Similarly, the O-model exhibits a consistent increase in the number of selected sensors from 11 sensors at 20 % to 24 sensors at 100 %, representing an improvement. The (t, n)-model follows suit with an improvement in the number of selected sensors, ranging from 13 at 20 % to 26 at 100 % search rate. In contrast, our MWG-QDRL-IPDO model shows efficient and optimized sensor selection process. Despite the ascending sensor search rate, there is an improvement in the number of selected sensors, ranging from 15 at 20 % to 28 at 100 %. This underscores the efficiency of the MWG-QDRL-IPDO model in optimizing sensor deployment for Soil EC monitoring, shows a more resource-efficient approach compared to the existing models.

In Fig. 9, a comprehensive comparison of accuracy for the Soil EC sensor case is presented among different models. For the R-model, there is a consistent increase in accuracy as the sensor search rate escalates, ranging from 75.89 % at 20 % search rate to 83.52 % at 100 %, indicating an improvement. Similarly, the O-model exhibits a continuous increase in accuracy improvement from 79.58 % at 20 % to 87.21 % at 100 %. The (t, n)-model follows suit with an improvement in accuracy, ranging from 83.27 % at 20 % to 90.90 % at 100 % search rate. In contrast, our MWG-QDRL-IPDO model shows remarkable accuracy, with accuracy an improvement. The accuracy ranges from 86.96 % at 20 % to an impressive 94.58 % at 100 % search rate. This emphasizes the superior accuracy of the MWG-QDRL-IPDO model for Soil EC monitoring compared to existing models.

In Fig. 10, a detailed comparison of processing time for the Soil EC sensor case is presented among different models. For the R-model, there is an increase in processing time as the sensor search rate escalates, ranging from 43,500 ms at 20 % search rate to 47,500 ms at 100 %, indicating an improvement. Similarly, O-model exhibits an incremental trend in processing time from 33,500 ms at 20 % to 37,500 ms at 100 %, representing an improvement. The (t, n)-model follows suit with an improvement in processing time, ranging from 23,500 ms at 20 % to

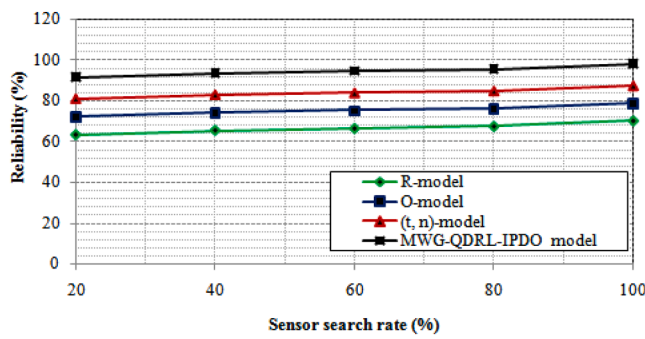


Fig. 11. Reliability comparison for Soil EC sensor case.

27,500 ms at 100 % search rate. In contrast, our MWG-QDRL-IPDO model shows a more efficient and optimized processing time. Despite the ascending sensor search rate, there is an improvement in processing time, ranging from 13,500 ms at 20 % to 17,500 ms at 100 %. This underscores the efficiency of MWG-QDRL-IPDO model in optimizing processing time for Soil EC monitoring, shows a more resource-efficient

approach compared to the existing models.

In Fig. 11, a comprehensive comparison of reliability for the Soil EC sensor case is depicted among different models. For the R-model, there is a consistent increase in reliability as the sensor search rate escalates, ranging from 63.34 % at 20 % search rate to 70.06 % at 100 %, indicating an improvement. Similarly, the O-model exhibits a continuous increase in reliability from 72.03 % at 20 % to 78.75 % at 100 %, representing an improvement. The (t, n)-model follows suit with an improvement in reliability, ranging from 80.72 % at 20 % to 87.44 % at 100 % search rate. In contrast, our MWG-QDRL-IPDO model shows a substantial increase in reliability, with reliability experiencing an improvement. The reliability ranges from 91.41 % at 20 % to an impressive 98.13 % at 100 % search rate. This emphasizes the superior reliability of the MWG-QDRL-IPDO model for Soil EC monitoring compared to existing models.

5.2. Comparative analysis with respect to precision agriculture

Table 3 provides a comprehensive comparison of measurement values and monitoring efficiency for proposed and existing precision

Table 3

Measurement values and monitoring efficiency comparison of proposed and existing precision agriculture models with varying IoT sensor nodes.

Model	IoT sensor nodes									
	10	20	30	40	50	10	20	30	40	50
	Measurement value (%)					Monitoring efficiency (%)				
R-model	57.15	58.23	59.24	60.41	62.53	78.05	78.65	78.88	79.07	79.20
O-model	63.39	64.46	65.48	66.65	68.76	83.91	84.51	84.73	84.93	85.06
(t, n)-model	69.62	70.70	71.71	72.88	75.00	89.77	90.37	90.59	90.79	90.92
MWG-QDRL-IPDO model	75.86	76.93	77.95	79.12	81.23	95.63	96.23	96.45	96.65	96.78

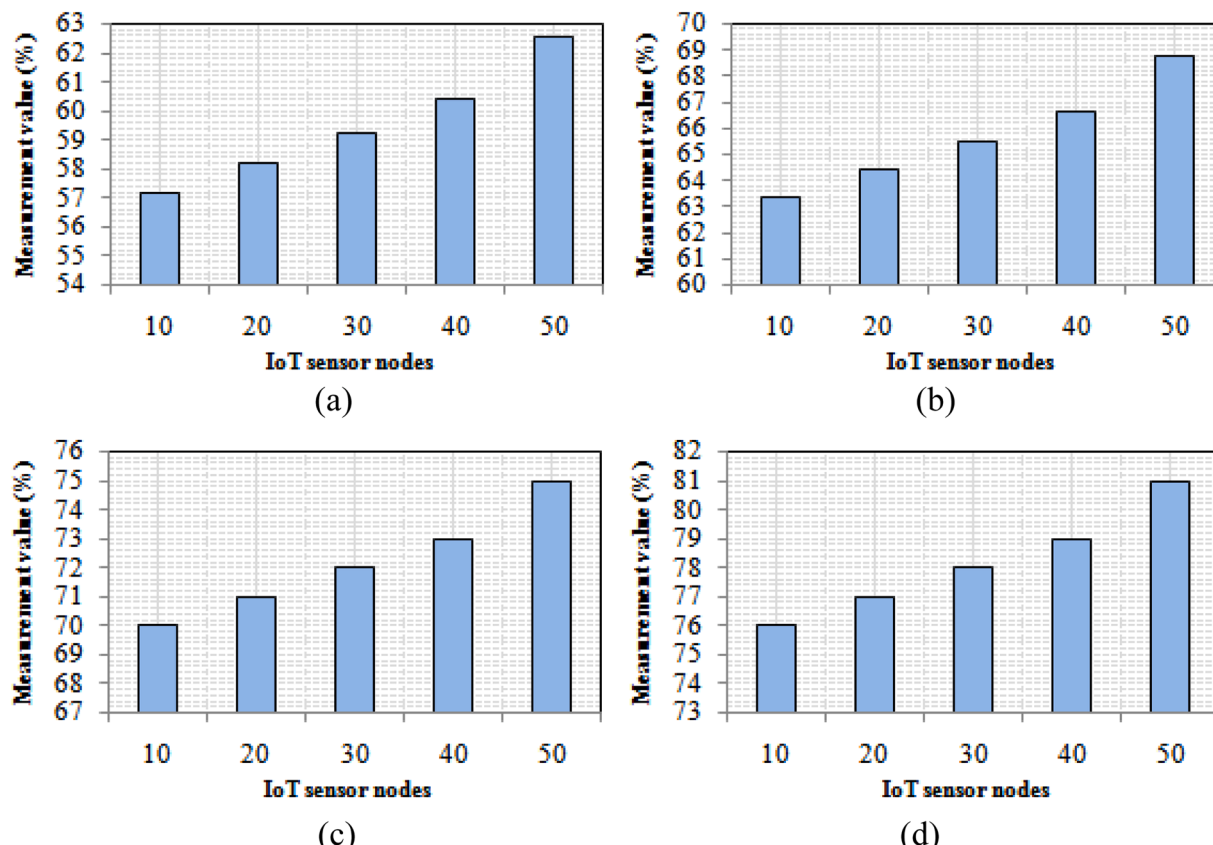


Fig. 12. Measurement values comparison of proposed and existing precision agriculture models with varying IoT sensor nodes for (a) R-model (b) O-model (c) (t, n)-model (d) MWG-QDRL-IPDO model.

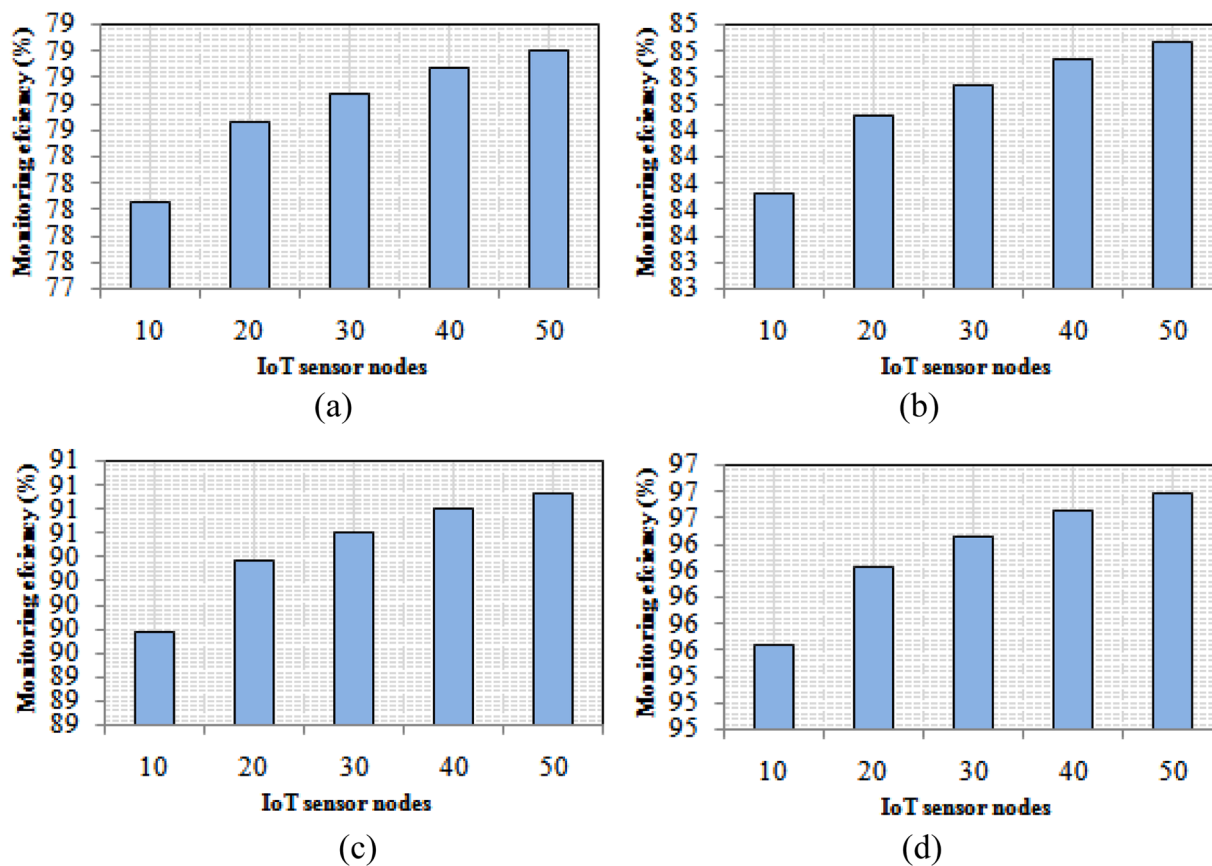


Fig. 13. Monitoring efficiency comparison of proposed and existing precision agriculture models with varying IoT sensor nodes for (a) R-model (b) O-model (c) (t, n)-model (d) MWG-QDRL-IPDO model.

agriculture models with varying IoT sensor nodes. In Fig. 12, we showed a comparison of measurement values for proposed and existing precision agriculture models.

The amount of IoT sensor bulges is diverse from 10 to 50, with each model's corresponding measurement values provided. For the R-model, there is a gradual increase in measurement values as the number of IoT sensor nodes rises, ranging from 57.15 % with 10 nodes to 62.53 % with 50 nodes, indicating an improvement. Similarly, the O-model exhibits a consistent increase in measurement values from 63.39 % with 10 nodes to 68.76 % with 50 nodes, representing an improvement. The (t, n)-model follows suit with an improvement in measurement values, ranging from 69.62 % with 10 nodes to 75 % with 50 nodes. In contrast, our proposed MWG-QDRL-IPDO model showcases a more efficient and optimized measurement value progression. Despite the increasing number of IoT sensor nodes, there is an improvement in measurement values, ranging from 75.86 % with 10 nodes to 81.23 % with 50 nodes. This underscores the efficiency of the MWG-QDRL-IPDO model in optimizing measurement values for precision agriculture, shows resource-efficient approach compared to the existing models.

In Fig. 13, a detailed comparison of monitoring efficiency for

proposed and existing precision agriculture models is presented with varying IoT sensor nodes across. For the R-model, there is a marginal increase in monitoring efficiency as the number of IoT sensor nodes increases, ranging from 78.05 % with 10 nodes to 79.21 % with 50 nodes, indicating an improvement. Similarly, the O-model exhibits a gradual increase in monitoring efficiency from 83.91 % with 10 nodes to 85.06 % with 50 nodes, representing an improvement. The (t, n)-model follows suit with an improvement in monitoring efficiency, ranging from 89.77 % with 10 nodes to 90.20 % with 50 nodes. In contrast, our proposed MWG-QDRL-IPDO model shows consistently high monitoring efficiency. Despite the increasing number of IoT sensor nodes, there is a slight improvement in monitoring efficiency, ranging from 95.63 % with 10 nodes to 96.78 % with 50 nodes. This underscores the efficiency and stability of the MWG-QDRL-IPDO model in maintaining high monitoring efficiency for precision agriculture applications compared to the existing models.

Table 4 presents a comprehensive comparison of measurement values and monitoring efficiency for proposed and existing precision agriculture models across varying field areas (in acres). In Fig. 14, a detailed comparison of measurement values for proposed and existing

Table 4

Measurement values and monitoring efficiency comparison of proposed and existing precision agriculture models with varying field area (acre).

Model	Field area (acre)					Monitoring efficiency (%)				
	10	20	30	40	50	10	20	30	40	50
	Measurement value (%)									
R-model	52.41	52.86	53.19	53.33	53.45	72.54	72.97	73.12	73.21	73.24
O-model	58.65	59.09	59.42	59.56	59.68	78.40	78.82	78.98	79.07	79.10
(t, n)-model	64.88	65.33	65.66	65.80	65.92	84.26	84.68	84.83	84.92	84.96
MWG-QDRL-IPDO model	71.12	71.56	71.89	72.03	72.15	90.12	90.54	90.69	90.78	90.82

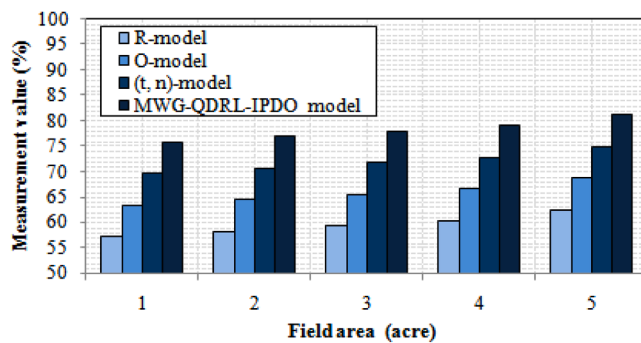


Fig. 14. Measurement values comparison of proposed and existing precision agriculture models with varying field areas.

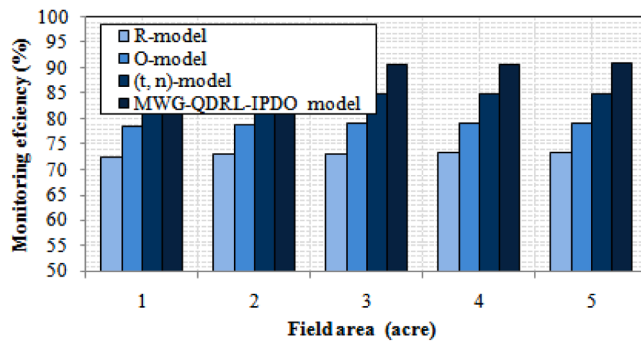


Fig. 15. Monitoring efficiency comparison of proposed and existing precision agriculture models with varying field areas.

precision agriculture models is illustrated across varying field areas. For the R-model, there is a gradual increase in measurement values as the field area expands, ranging from 52.41 % at 1 acre to 53.45 % at 5 acres, indicating an improvement. Similarly, the O-model exhibits a consistent increase in measurement values from 58.65 % at 1 acre to 59.68 % at 5 acres, representing an improvement. The (t, n)-model follows suit with an improvement in measurement values, ranging from 64.88 % at 1 acre to 65.92 % at 5 acres. In contrast, our proposed MWG-QDRL-IPDO model shows a more efficient and optimized measurement value progression. Despite the expanding field area, there is an improvement in measurement values, ranging from 71.12 % at 1 acre to 72.15 % at 5 acres. This underscores the efficiency of the MWG-QDRL-IPDO model in optimizing measurement values for precision agriculture, shows more resource-efficient approach compared to the existing models.

In Fig. 15, a comprehensive comparison of monitoring efficiency for proposed and existing precision agriculture models is presented with varying field areas. For the R-model, there is a marginal increase in monitoring efficiency as the field area expands, ranging from 72.54 % at 1 acre to 73.24 % at 5 acres, indicating an improvement. Similarly, the O-model exhibits a gradual increase in monitoring efficiency from 78.41 % at 1 acre to 79.11 % at 5 acres, representing an improvement. The (t, n)-model follows suit with an improvement in monitoring efficiency, ranging from 84.27 % at 1 acre to 84.97 % at 5 acres. In contrast, our MWG-QDRL-IPDO model shows a consistently high monitoring efficiency. Despite the expanding field area, there is a slight improvement in monitoring efficiency, ranging from 90.13 % at 1 acre to 90.83 % at 5 acres. This underscores the efficiency and stability of the proposed MWG-QDRL-IPDO model in maintaining high monitoring efficiency for precision agriculture applications compared to the existing models.

6. Conclusion

Our proposed smart optimal prediction model for sensors, rooted in

IoT-enabled precision agriculture, demonstrates multifaceted approach to enhance agricultural practices. Commencing with the refinement of the THAM index is using the modified Wild Geese (MWG) algorithm. The quantum deep reinforcement learning (QDRL) is used to compute the optimal sensor count for efficient coverage and improved communication within the agricultural field. The improved prairie dog optimization (IPDO) algorithm is used to optimizes the fertilizer regulatory measures. The MWG-QDRL-IPDO model displays a noteworthy trend of decreasing measurement values with escalating influencing factors, shows its efficiency and adept resource optimization. The numerical findings attest to MWG-QDRL-IPDO model's exceptional monitoring efficiency, which only experiences a slight decrease even in scenarios of expanding field areas. Notably, the model excels in sensor deployment optimization, necessitating sensors for effective coverage, thereby contributing significantly to its overall efficiency. In future, extending the application of the model to diverse crop types and geographical regions would provide insights into its adaptability and effectiveness across different agricultural settings. Collaborative efforts with agricultural stakeholders and industry partners can essential to validate the model's performance under real-world conditions and ensure its seamless integration into agricultural operations.

CRediT authorship contribution statement

Praveen Sankarasubramanian: Writing – review & editing, Writing – original draft, Visualization, Validation, Supervision, Software, Resources, Project administration, Methodology, Conceptualization.

Declaration of competing interest

The authors declare that they have no known competing financial interests or personal relationships that could have appeared to influence the work reported in this paper.

Ethics Statement

Not applicable: This manuscript does not include human or animal research. If this manuscript involves research on animals or humans, it is imperative to disclose all approval details.

Data availability

No data was used for the research described in the article.

References

- [1] O. Elijah, T.A. Rahman, I. Orikumhi, C.Y. Leow, M.N. Hindia, An overview of Internet of Things (IoT) and data analytics in agriculture: benefits and challenges, *IEEE Int. Things J* 5 (5) (2018) 3758–3773.
- [2] N. Ahmed, D. De, I. Hussain, Internet of Things (IoT) for smart precision agriculture and farming in rural areas, *IEEE Int. Things J* 5 (6) (2018) 4890–4899.
- [3] W.L. Chen, Y.B. Lin, Y.W. Lin, R. Chen, J.K. Liao, F.L. Ng, Y.Y. Chan, Y.C. Liu, C. C. Wang, C.H. Chiu, T.H. Yen, AgriTalk: IoT for precision soil farming of turmeric cultivation, *IEEE Int. Things J* 6 (3) (2019) 5209–5223.
- [4] G.A. Taylor, H.B. Torres, F. Ruiz, M.N. Marin, D.M. Chaves, L.T. Arboleda, C. Parra, H. Carrillo, A.M. Mouazen, pH measurement IoT system for precision agriculture applications, *IEEE Lat. Am. Transac* 17 (05) (2019) 823–832.
- [5] A. Goap, D. Sharma, A.K. Shukla, C.R. Krishna, An IoT based smart irrigation management system using Machine learning and open source technologies, *Comp. Electr. Agricul* 155 (2018) 41–49.
- [6] A. Khanna, S. Kaur, Evolution of Internet of Things (IoT) and its significant impact in the field of precision agriculture, *Comp. Electr. Agricul* 157 (2019) 218–231.
- [7] R. Dhall, H. Agrawal, An improved energy efficient duty cycling algorithm for IoT based precision agriculture, *Proced. Comp. Sci* 141 (2018) 135–142.
- [8] K. Foughali, K. Fathallah, A. Frihida, Using Cloud IOT for disease prevention in precision agriculture, *Proced. Comp. Sci* 130 (2018) 575–582.
- [9] M.S. Mekala, P. Viswanathan, CLAY-MIST: IoT-cloud enabled CMM index for smart agriculture monitoring system, *Measurement*, 134 (2019) 236–244.
- [10] A. Moon, J. Kim, J. Zhang, S.W. Son, Evaluating fidelity of lossy compression on spatiotemporal data from an IoT enabled smart farm, *Comp. Electr. Agricul* 154 (2018) 304–313.

- [11] A. Khattab, S.E. Habib, H. Ismail, S. Zayan, Y. Fahmy, M.M. Khairy, An IoT-based cognitive monitoring system for early plant disease forecast, *Comp. Electr. Agricul* 166 (2019) 105028.
- [12] B. Mazon-Olivo, D. Hernández-Rojas, J. Maza-Salinas, A. Pan, Rules engine and complex event processor in the context of internet of things for precision agriculture, *Comp. Electr. Agricul* 154 (2018) 347–360.
- [13] B. Keswani, A.G. Mohapatra, A. Mohanty, A. Khanna, J.J. Rodrigues, D. Gupta, V.H.C. De Albuquerque, Adapting weather conditions based IoT enabled smart irrigation technique in precision agriculture mechanisms, *Neur. Comput. Applic* 31 (2019) 277–292.
- [14] X. Feng, F. Yan, X. Liu, Study of wireless communication technologies on Internet of Things for precision agriculture, *Wirel. Pers. Commun* 108 (3) (2019) 1785–1802.
- [15] S.S. Koshy, V.S. Sunnam, P. Rajgarhia, K. Chinnusamy, D.P. Ravulapalli, S. Chunduri, Application of the internet of things (IoT) for smart farming: a case study on groundnut and castor pest and disease forewarning, *CSI Transac. ICT* (6) (2018) 311–318.
- [16] S. AlZu'bi, B. Hawashin, M. Mujahed, Y. Jararweh, B.B. Gupta, An efficient employment of internet of multimedia things in smart and future agriculture, *Multim. Tools Applic* 78 (2019) 29581–29605.
- [17] D. Thakur, Y. Kumar, A. Kumar, P.K. Singh, Applicability of wireless sensor networks in precision agriculture: a review, *Wirel. Person. Commun* 107 (2019) 471–512.
- [18] H. Ibrahim, N. Mostafa, H. Halawa, M. Elsalamouny, R. Daoud, H. Amer, Y. Adel, A. Shaarawi, A. Khattab, H. ElSayed, A layered IoT architecture for greenhouse monitoring and remote control, *SN Appl. Sci* 1 (2019) 1–12.
- [19] M.C. Vuran, A. Salam, R. Wong, S. Irmak, Internet of underground things in precision agriculture: architecture and technology aspects, *Ad Hoc Netw* 81 (2018) 160–173.
- [20] Q. Kong, K. Kuriyan, N. Shah, M. Guo, Development of a responsive optimisation framework for decision-making in precision agriculture, *Comp. Chem. Eng* 131 (2019) 106585.
- [21] H. Agrawal, R. Dhall, K.S.S. Iyer, V. Chetlapalli, An improved energy efficient system for IoT enabled precision agriculture, *J. Amb. Intel. Human. Comput* 11 (2020) 2337–2348.
- [22] M. Jayalakshmi, V. Gomathi, Sensor-cloud based precision agriculture approach for intelligent water management, *Int. J. Plant Produc* 14 (2020) 177–186.
- [23] K.R. Gsangaya, S.S.H. Hajjaj, M.T.H. Sultan, L.S. Hua, Portable, wireless, and effective internet of things-based sensors for precision agriculture, *Int. J. Environ. Sci. Technol* 17 (2020) 3901–3916.
- [24] N. Lin, X. Wang, Y. Zhang, X. Hu, J. Ruan, Fertigation management for sustainable precision agriculture based on Internet of Things, *J. Clean. Produc* 277 (2020) 124119.
- [25] N. Gupta, M. Khosravy, N. Patel, N. Dey, S. Gupta, H. Darbari, R.G. Crespo, Economic data analytic AI technique on IoT edge devices for health monitoring of agricultural machines, *Appl. Intel* 50 (2020) 3990–4016.
- [26] N.G. Rezk, E.E.D. Hemdan, A.F. Attia, A. El-Sayed, M.A. El-Rashidy, An efficient IoT based smart farming system using machine learning algorithms, *Multim. Tools Applic* 80 (2021) 773–797.
- [27] F. Akhter, H.R. Siddiquei, M.E.E. Alahi, S.C. Mukhopadhyay, Design and development of an IoT-enabled portable phosphate detection system in water for smart agriculture, *Sens. Actuat. A: Phys* 330 (2021) 112861.
- [28] T. Anand, S. Sinha, M. Mandal, V. Chamola, F.R. Yu, AgriSegNet: Deep aerial semantic segmentation framework for IoT-assisted precision agriculture, *IEEE Sens. J* 21 (16) (2021) 17581–17590.
- [29] S.K. Roy, S. Misra, N.S. Raghuwanshi, S.K. Das, AgriSens: IoT-based dynamic irrigation scheduling system for water management of irrigated crops, *IEEE Int. Things J* 8 (6) (2020) 5023–5030.
- [30] S. Atalla, S. Tarapiah, A. Gawanmeh, M. Daradkeh, H. Mukhtar, Y. Himeur, W. Mansoor, K.F.B. Hashim, M. Daadoo, IoT-enabled precision agriculture: developing an ecosystem for optimized crop management, *Information* 14 (4) (2023) 205.
- [31] M.S. Mekala, P. Viswanathan, (t,n): sensor stipulation with THAM index for smart agriculture decision-making IoT system, *Wirel. Person. Commun* 111 (3) (2020) 1909–1940.
- [32] L. Garcia, L. Parra, J.M. Jimenez, J. Lloret, P.V. Mauri, P. Lorenz, DronAway: A proposal on the use of remote sensing drones as mobile gateway for WSN in precision agriculture, *Appl. Sci* 10 (19) (2020) 6668.
- [33] S. Petkovic, D. Petkovic, A. Petkovic, IoT devices VS. drones for data collection in agriculture, *DAAAM Int. Scient. Book* 16 (2017) 63–80.